Carbonaceous species in PM2.5 and PM10 in urban area of Zhengzhou in China: Seasonal variations and source apportionment

Qun Wang, Nan Jiang, Shasha Yin, Xiao Li, Fei Yu, Yue Guo, Ruiqin Zhang

PII: S0169-8095(16)30239-3
DOI: doi: 10.1016/j.atmosres.2017.02.003
Reference: ATMOS 3880

To appear in: *Atmospheric Research*

Received date: 13 August 2016
Revised date: 28 January 2017
Accepted date: 1 February 2017

Please cite this article as: Qun Wang, Nan Jiang, Shasha Yin, Xiao Li, Fei Yu, Yue Guo, Ruiqin Zhang , Carbonaceous species in PM2.5 and PM10 in urban area of Zhengzhou in China: Seasonal variations and source apportionment. The address for the corresponding author was captured as affiliation for all authors. Please check if appropriate. Atmos(2017), doi: 10.1016/j.atmosres.2017.02.003

Carbonaceous species in $PM_{2.5}$ and PM_{10} in urban area of Zhengzhou in China: seasonal variations and source apportionment

Qun Wang, Nan Jiang, Shasha Yin, Xiao Li, Fei Yu, Yue Guo, Ruiqin Zhang[1]

College of Chemistry and Molecular Engineering, Research Institute of Environmental Science, Zhengzhou University, Zhengzhou 450001, China

Abstract:

$PM_{2.5}$ and PM_{10} samples were simultaneously collected in an urban site in Zhengzhou, China from October 2014 to July 2015 representing the four seasons. Organic carbon (OC), elemental carbon (EC), and non-polar organic compounds including n-alkanes (C_8–C_{40}) and polycyclic aromatic hydrocarbons (PAHs) were quantified. The characteristics of their concentrations, seasonal variations, and sources of n-alkanes and PAHs were investigated. Diagnostic ratios and positive matrix factorization (PMF) were used to characterize carbonaceous species, identify their possible sources, and apportion the contributions from each possible source. The concentrations of the components exhibited distinct seasonal variation, that is, the concentrations are high in winter and low in summer. This finding could be associated with increase in air pollutant emissions during heating season and stable weather condition. The estimated total carbonaceous aerosol accounts for 32% of $PM_{2.5}$ and 30% of PM_{10}. Hence, carbonaceous compounds were the major components of particulate matter in the study area. Moreover, OC, EC, PAHs, and n-alkanes preferentially accumulated into fine particles. The carbonaceous components exhibited high correlation in $PM_{2.5}$ and PM_{10}, thereby indicating that their sources were similar. The PMF results revealed that the main sources of PAHs were coal combustion (40%) and motor vehicles (29%); n-alkanes were mainly from burning of fossil fuel (48%). These sources were consistent with the diagnostic ratios obtained. This study provides guidance for improving air quality and reducing human exposure to toxic air

[1] Corresponding author. Tel: 1-370-371-7002; Fax: 0371-67781163

E-mail address: rqzhang@zzu.edu.cn

pollutants.

Keywords: $PM_{2.5}$; PM_{10}; PAHs; n-alkanes; PMF; Zhengzhou

1. Introduction

Particulate matter (PM) pollution is a serious environmental concern in most areas in China because of rapid industrialization and urbanization (Huang et al., 2014). Carbonaceous aerosol, which accounts for 20%–50% of $PM_{2.5}$, negatively influences visibility, climate system, and human health (Paraskevopoulou et al., 2015). Carbonaceous aerosol is classified into elemental carbon (EC) and organic carbon (OC). EC is an important light-absorbing component in the atmosphere and is produced from incomplete combustion of carbon-containing materials (Jacobson, 2001). OC consists of thousands of organic compounds and is derived from primary emissions (primary OC), such as coal combustion, vehicular exhaust, and biomass burning (Zhang et al., 2008); OC is also produced by secondary formation (secondary OC, SOC) through gas-to-particle conversion of volatile organic compounds (VOCs) in the atmosphere (Satsangi et al., 2012).

Polycyclic aromatic hydrocarbon (PAHs) and n-alkanes are important non-polar classes of organic compounds. PAHs are categorized as a class of persistent organic pollutants because of their potential toxicity, carcinogenicity, and mutagenicity; PAHs are mainly derived from coal burning, motor vehicle exhausts, heat and power generation and biomass burning (Bi et al., 2003； Rajput et al., 2011). n-Alkanes are emitted from both anthropogenic (e.g., fossil fuel combustion and biomass burning) and biogenic sources (e.g., higher plant waxes) (Bi et al., 2002). Identifying the sources of PAHs and n-alkanes can formulate effective control strategies to reduce organic contamination.

Positive matrix factorization (PMF) is an advanced factor analysis tool based on the least-squares minimization algorithm (Paatero and Unto, 1994). PMF utilizes error estimates and integrates non-negativity constraints into optimization and is thus widely applied to PM source appointment (Zhang et al., 2009; Chan et al., 2011). PMF is also

used to investigate sources of PAHs and n-alkanes (Okuda et al., 2010; Moeinaddini et al., 2014; Callén et al., 2014).

A number of scholars have investigated the characteristics of carbonaceous aerosol worldwide (Castro et al., 1999; Duarte et al., 2008; Cao et al., 2013; Wang et al., 2015a). These studies assist the government to design effective air pollution control measures for improving air quality. The Central Plains Economic Region (CPER) is an emerging economic center in central China; this region accounts for 8.9% of the national GDP and 10.9% of the national population in 2015. The air quality in this region has become increasingly deteriorated. Zhengzhou, the capital of Henan Province and the core city of the CPER, has experienced serious air pollution problems (Tao et al., 2014a). However, only few studies have reported the air quality in Zhengzhou; these studies mainly discussed source apportionment and seasonal variations of $PM_{2.5}$ (Geng et al., 2013; Wang et al., 2014). Moreover, carbonaceous components have been rarely investigated in this area. Hence, the characteristics of carbonaceous components in $PM_{2.5}$ and PM_{10} must be elucidated.

This study mainly aims to (1) analyze the pollution levels and seasonal characteristics of carbonaceous components [OC, EC, n-alkanes (C_8–C_{40}), and 16 priority PAHs] in $PM_{2.5}$ and PM_{10}; (2) investigate the relationship of carbonaceous components between $PM_{2.5}$ and PM_{10}; and (3) identify potential pollution sources of PAHs and n-alkanes through PMF. These results hope to provide sound basis for effective control of urban atmospheric aerosol pollution.

2. Materials and methods

2.1 Sampling

The sampling site is located in the new campus of Zhengzhou University (34°48′ N; 113°31′ E), adjacent to the fourth-ring road in the west. Samplers were installed on the roof of a four-storey building (about 13 m above ground level). Figure. 1 shows the sampling site in relation to Henan Province and China. Zhengzhou experiences temperate continental monsoon climate with four clearly distinct seasons. Table 1

shows the meteorological parameters provided by Henan Province Meteorology Bureau during the sampling period. These parameters include wind speed, relative humidity, air pressure, and air temperature. During the sampling period, the average temperatures are 17.4 °C, 5.1 °C, 12.9 °C, and 26.4 °C; the relative humidity levels are 60%, 47%, 55%, and 67%; and the wind speeds are 2.2, 2.1, 2.7, and 1.7 for autumn, winter, spring, and summer, respectively. The atmospheric pressure is higher in winter than that in the other seasons.

A total of 61 $PM_{2.5}$ and 53 PM_{10} samples (eight PM_{10} samples were rejected because of instrument failure) were collected in four months (i.e., October 2014, January, April, and July 2015; representing the four seasons). The sampling time was 23 h, starting at 9:00 in the morning and ends at 8:00 the following morning. $PM_{2.5}$ and PM_{10} samples were collected simultaneously on quartz microfiber filters (20.3 cm × 25.4 cm, Pall, USA) by using two high-volume (flow rate 1.13 m^3 min^{-1}) samplers (TE-6070D, Tisch Environment, USA).

Before sampling, quartz filters were baked at 450 °C in a muffle furnace for 5 h to remove the adsorbed organic materials. The filters were stabilized in a clean room (25 ± 0.5 °C, 50% ± 2% relative humidity) for 48 h before and after sampling and weighed using a microbalance with a resolution of 10 μg (Mettler Toledo XS205, Switzerland). Before analysis, the filters were stored at −20 °C.

2.2 Analytical procedure

OC and EC were analyzed through thermal/optical transmittance method (Birch and Cary, 1996) using a sunset semi-continuous OC/EC analyzer. Additional details were described in our previous study (Geng et al., 2013).

Each sample was extracted twice through pressurized liquid extraction using an accelerated solvent extractor (ASE350, Dionex, USA) to determine the mass concentrations of PAHs and n-alkanes. The sampled filter was cut into pieces, with an area of 10.9 cm^2, and placed in 34 mL of ASE extraction cells. Briefly, 20 μL of the PAH surrogate internal standard mixture (p-terphenyl-d_{14} and 2-fluorobiphenyl) were

spiked to estimate loss during the process. The cells were filled with dichloromethane/hexane (1:1 v/v), pressurized to 1.5 MPa, and heated to 100 °C within 5 min. The temperature was held constant for 5 min, and the cells were purged with high-purity nitrogen for 90 s. The extracts were concentrated with a rotary vacuum evaporator and condensed to 1 mL under high-purity nitrogen flow. Briefly, 20 μL of five deuterated-PAH standard mixtures (naphthalene-D_8, acenaphthene-D_{10}, phenanthrene-D_{10}, chrysene-D_{12} and perylene-D_{12}) were added to the extracts prior to GC-MS analysis.

PAHs and n-alkanes were analyzed using Agilent 7890A gas chromatograph (GC) fitted with a DB-5MS capillary column (30 m × 0.25 mm × 0.25 μm), coupled to a 5975C mass-selective detector. For PAH analysis, the oven temperature was initially set at 70 °C for 2 min. The temperature was increased to 320 °C at a rate of 10 °C min^{-1}, held for 5 min. For n-alkane analysis, the initial oven temperature was set at 40 °C, held for 10 min and increased to 320 °C at a rate of 6 °C min^{-1}, held for 15 min. Selected ion monitoring was used to analyze PAHs and n-alkanes. The concentrations of PAHs and n-alkanes were quantified using internal standard and external standard methods, respectively.

2.3 Quality assurance and control (QA/QC)

All analytical procedures were monitored with strict quality assurance and quality control measures. Blank filters were analyzed, and the results were corrected for the average of the blank concentration, that is, 0.5 μg m^{-3} for OC; EC, PAHs, and n-alkanes were not detected in the blank samples. The precision of the analysis was estimated by calculating %RSD of the selected samples analyzed for seven times. The RSDs are < 5% for PAHs and n-alkanes. Method detection limit (MDL) is defined as three times the mean of the standard deviation obtained from seven consecutive analyses of the lowest point of the curve. The MDL for both EC and OC is 0.2 μg m^{-3}. The MDLs for the target PAHs and n-alkanes are 0.07–0.91 and 0.1–1.8 ng m^{-3}, respectively. The average recoveries are 71%–110% and 72%–116% for analyses of PAHs and

n-alkanes, respectively. The correlation coefficients (r^2) for linear regressions of the calibration curves are over 0.995.

2.4 PMF modeling

PMF is a receptor model based on chemical characterization of collected particles that can identify potential source categories and source contributions when the source profiles are not known. PMF can decompose a matrix of sample data (X) into two matrices: the source profile matrix (F) and the source contribution matrix (G) (Eq. (1)) (Paatero and Tapper, 1994).

$$x_{ij}=\sum_{k=1}^{p} g_{ik} f_{kj} + e_{ij} \quad (1)$$

where x_{ij} is the concentration of the j^{th} species measured in the i^{th} sample, p is the number of factors contributing to the samples, g_{ik} is the contribution of the k^{th} source in the i^{th} sample and f_{jk} is the concentration of the j^{th} species in k^{th} source, and e_{ij} is the error of the PMF model for the j^{th} species measured on the i^{th} sample.

The objective of PMF model is to minimize Q function by using a weighted least squares method, which is defined as:

$$Q=\sum_{i=1}^{m}\sum_{j=1}^{n}(e_{ij}/u_{ij}) \quad (2)$$

where u_{ij} is an estimate of the uncertainty in the j^{th} species determined in the i^{th} sample, which is applied to weight the observations that contain sampling errors, detection limits, missing data and outliers.

The details of PMF have been described in the PMF 5.0 User Guide (USEPA, 2014). The input data files include sample species concentration and sample species uncertainty. The uncertainty for sample species was calculated by concentration and MDL. Concentrations below the MDL were replaced by MDL/2, uncertainties were assumed to be (0.2concentration + MDL/3) and concentrations above the MDL, uncertainties were assumed to be (0.2concentration + MDL/3) (Jang et al., 2013). Species with signal-to-noise below 2 were defined as weak variables (Paatero and

Hopke, 2003). The base model was run to produce primary PMF output of profiles and contribution. The rotational freedom parameter (Fpeak) function were used to control the rotational ambiguity. To obtain the optical number of sources, 2-5 factors were examined. The model was run 100 times with a random seed. The Q values, the resulting source profiles, and the scaled residuals distributions were studied to get the best factor solution. The detailed PMF diagnostic are shown in supplemental material.

3. Results and discussion

3.1 PM mass concentrations and variations of OC and EC

The seasonal concentrations of $PM_{2.5}$, PM_{10}, OC, and EC are summarized in Table 2. The daily concentrations of OC, EC, and PM during the sampling period are shown in Fig. 2. With $PM_{2.5}$ mass concentrations ranged from 58 μg m^{-3} to 353 μg m^{-3} (average: 146 ± 59 μg m^{-3}), and the PM_{10} ranged from 102 μg m^{-3} to 412 μg m^{-3} (average: 214 ± 68 μg m^{-3}), most daily concentrations were higher than the Chinese National Ambient Air Quality Standards of grade 2 ($PM_{2.5}$: 75 μg m^{-3} and PM_{10}: 150 μg m^{-3}). The seasonal variations were evident; the highest concentrations were found in winter ($PM_{2.5}$: 179 ± 90 μg m^{-3}, PM_{10}: 263 ± 73 μg m^{-3}), followed by autumn ($PM_{2.5}$: 154 ± 41 μg m^{-3}, PM_{10}: 252 ± 71 μg m^{-3}), spring ($PM_{2.5}$: 147 ± 31 μg m^{-3}, PM_{10}: 202 ± 47 μg m^{-3}), and summer ($PM_{2.5}$: 102 ± 22 μg m^{-3}, PM_{10}: 164 ± 42 μg m^{-3}). The ratio of $PM_{2.5}/PM_{10}$ ranged from 0.38 to 0.80, with an annual average of 0.66. This result indicated that PM_{10} was dominated by $PM_{2.5}$ during the sampling period in the present study site.

The OC concentrations in $PM_{2.5}$ were 25, 45, 22, and 12 μg m^{-3}, which accounted for 68%, 76%, 79%, and 55% of OC in PM_{10} (37, 59, 28, and 22 μg m^{-3}), in autumn, winter, spring, and summer, respectively. The analog numbers for EC in $PM_{2.5}$ (5, 17, 8, and 7 μg m^{-3}) were 71%, 57%, 73%, and 58% of EC in PM_{10} (7, 30, 11, and 12 μg m^{-3}) in each season. The results were consistent with Li et al. (2015), suggesting that EC and OC were enriched in small particles. OC concentrations exhibited similar seasonal pattern with that of PM, whereas EC concentrations showed weak seasonal variation but were high in winter. The high concentrations of EC, OC, and PM in

winter were mainly associated with increased coal consumption during heating season and unfavorable dispersion conditions. The OC and EC concentrations measured in Zhengzhou were compared with results from other cities. The mean concentrations of OC in PM_{10} and $PM_{2.5}$ in Zhengzhou (27 μg m^{-3} and 34 μg m^{-3}) were similar to those reported in Pune, India (32 μg m^{-3} and 34 μg m^{-3}) (Pipal and Gursumeeran Satsangi, 2015), higher than those in an urban area (13.8 μg m^{-3} and 13.1 μg m^{-3}) and a suburban site (5.7 μg m^{-3} in $PM_{2.5}$) in Nanjing, China (Li et al., 2015; Chen et al., 2017), and Baotou, China (21.8 μg m^{-3} and 15.8 μg m^{-3}) (Zhou et al., 2016). The mean concentrations of EC in PM_{10} and $PM_{2.5}$ in Zhengzhou were higher than these cities. This indicated the severity of carbonaceous components pollution in the Zhengzhou urban environment.

As shown in Table 2, the OC/EC ratios in $PM_{2.5}$ and PM_{10} were higher in autumn than those in spring, winter, and summer. The highest OC/EC ratio was found in autumn probably because of open biomass burning during harvest seasons in the study area. The correlation coefficients between OC and EC concentrations in $PM_{2.5}$ and PM_{10} were 0.872 ($P < 0.01$) and 0.932 ($P < 0.01$), respectively (Table 3). This finding indicated that OC and EC had common combustion sources.

OC/EC ratios exceeding 2.0 may indicate secondary organic aerosol formation (Chow et al., 1996). EC tracer method was applied to estimate the concentration of SOC, assuming that the minimum ratio of OC/EC was a constant mixture of primary OC (Castro et al., 1999). SOC was calculated as follows:

$$SOC = OC - (OC/EC)_{min} \quad (3)$$

The minimum OC/EC was simplified as the smallest ratio of OC to EC in each season (Li et al., 2015). The estimated SOC concentrations are presented in Table 2. The annual average SOC concentrations in $PM_{2.5}$ and PM_{10} were 12 and 19 μg m^{-3}, respectively, with the same seasonal variation in winter > autumn > spring > summer. The SOC/OC ratio in $PM_{2.5}$ was higher in autumn (0.44) and winter (0.37) than that in spring (0.36) and summer (0.32); this trend was similar to that in PM_{10}. The seasonal

variation in high SOC concentration and SOC/OC ratio in autumn and winter were consistent with previous observations in Beijing (Zhao et al., 2013). In the present study, the high levels of SOC and SOC/OC in autumn and winter can be attributed to increasing emissions of residential coal combustion and biomass burning, which could significantly contribute to gaseous precursors of SOC and lead to the high levels of SOC. In addition, meteorological conditions of thermal inversions and low planetary boundary layer height frequently occurred during autumn and winter in the present study area; these phenomena facilitated the accumulation of pollutants. Furthermore, low temperatures in winter accelerated the condensation of volatile organic compounds on particulate matter.

Total carbonaceous aerosol (TCA) was calculated by the sum of EC and organic matter estimated by multiplying the amount of OC by 1.6 to assess the contribution of carbonaceous aerosols to PM mass (Turpin and Lim, 2001). TCA accounted for an average of 32% of $PM_{2.5}$ and 30% of PM_{10}, with the same seasonal rank of winter > spring > autumn > summer. Compared to other sites, the obtained TCA/$PM_{2.5}$ ratios were higher than those reported by Zhou et al. (2016) in four cities of China (16%–23%); and lower than those in Agra, India (50.3%) (Pachauri et al., 2013), Guangzhou (32%–35%), and Hong Kong (43%–57%) (Duan et al., 2007). Hence, carbonaceous aerosol was an important component in $PM_{2.5}$ in Zhengzhou.

3.2 Seasonal variations of PAHs

Sixteen priority PAHs proposed by USEPA were measured in this study; these PAHs include naphthalene (Nap), acenaphthylene (Acy), acenaphthene (Ace), fluorene (Flu), phenanthrene (Phe), anthracene (Ant), fluoranthene (Flt), pyrene (Pyr), benz[a]anthracene (BaA), chrysene (Chr), benzo[b]fluoranthene (BbF), benzo[k]fluoranthene (BkF), benzo[a]pyrene (BaP), indeno[1,2,3-cd]pyrene (IcdP), dibenz[a,h]anthracene (DaA), and benzo[ghi]perylene (BghiP). The total PAH mass concentrations in $PM_{2.5}$ and PM_{10} were 9–338 (average: 58 ng m^{-3}) and 15–341 ng m^{-3} (average: 78 ng m^{-3}), respectively, showing the same trend of winter > autumn > spring >

summer (Table 4). The Σ_{16}PAHs concentration in winter (heating season) was significantly higher than in the other seasons. Particularly, the concentration was approximately 5-fold higher in winter than that in summer because of higher emissions (domestic heating, cold start of motor vehicle engines) and adverse weather conditions (low mixing-layer heights and horizontal wind speed) in the former. The ratio of $PM_{2.5\text{-PAHs}}/PM_{10\text{-PAHs}}$ was higher than 0.6 in the four seasons, revealing that most PAHs were associated with $PM_{2.5}$. The PAHs levels in the study area were higher than those in Guangzhou, China (17 ng m^{-3} in $PM_{2.5}$) (Gao et al., 2012); similar to those in Chengdu, China (37 ng m^{-3} in $PM_{2.5}$ and 41 ng m^{-3} in PM_{10}) (Shi et al., 2015); and lower than that in Zonguldak, Turkey (88 ng m^{-3} for $PM_{2.5}$ and 94 ng m^{-3} in PM_{10}) (Akyüz and Çabuk, 2009). Wang et al. (2015b) reported the 3-year average of Σ_{16}PAHs (174 ng m^{-3} in $PM_{2.5}$) in Zhengzhou from 2011 to 2013; the value was three times higher than that obtained in the present study. The reduced Σ_{16}PAH concentration might be associated with the random effects of meteorological condition and measures used to improve air quality (e.g., stricter emission control).

Figure 3 shows the seasonal variations in 16 individual PAHs (winter > autumn > spring > summer) during the sampling period. BbF, BkF, Chr, BaA, Ant, IcdP, and BghiP were abundant, accounting for 70% of PAHs in both $PM_{2.5}$ and PM_{10}. BaP, considered as the most carcinogenic substance, exhibited annual average concentrations of 3.3 ng m^{-3} in $PM_{2.5}$ and 5.6 ng m^{-3} in PM_{10}; these values were higher than the air quality guideline (1 ng m^{-3}) set by the World Health Organization (WHO 2000). Carcinogenic PAHs (CANPAHs) include BaA, Chr, BbF, BkF, BaP, IcdP, and DaA (He et al., 2014). The annual average concentrations of CANPAHs were 34 and 48 ng m^{-3}, accounting for 59% and 62% of PAHs in $PM_{2.5}$ and PM_{10}, respectively (Table 4). The health risk of PAHs can be assessed using BaP_{eq}, which is calculated by multiplying the PAH concentration with their corresponding toxic equivalent factor (Nisbet and LaGoy, 1992). The annual $\Sigma_{16}PAHs_{TEQ}$ values for $PM_{2.5}$ and PM_{10} were 6 and 9 ng m^{-3}, respectively. Thus, studies should be directed toward human health risk

identified in the study area.

The 16 PAHs evaluated can be classified into three groups: those with 2–3 ring (Nap, Acy, Ace, Flu, Phe, and Ant), 4 ring (Flt, Pyr, BaA, and Chr), and 5–6 ring (BbF, BkF, BaP, IcdP, DaA, and BghiP). As shown in Fig. 4, the relative contributions of PAHs with different ring sizes varied in each season. The contributions of PAHs with different rings were similar between PM_{10} and $PM_{2.5}$; 4 ring > 5–6 ring > 2–3 ring (winter) and 5–6 ring > 4 ring > 2–3 ring (other three seasons). PAHs with 2–3 ring constitute only a small part (less than 20%), whereas PAHs with 4–6 ring dominated in the Σ_{16}PAHs. PAHs with 2–3 ring exhibited the lowest proportion (9%) in summer and the highest (21%) in winter. This finding could be due to partitioning of PAHs with few rings in the gas phase at high temperatures and strong solar radiation in summer (Bi et al., 2003). Conversely, PAHs with few rings were more likely to load on particle phase, resulting in high concentrations under relatively low temperature and weak solar radiation in winter. The proportion of PAHs with 4 ring was high in winter (48%) and low in summer (29%), whereas that of PAHs with 5–6 ring was the highest in winter (61%). This finding is due to the fact that 4 ring PAHs are semi-volatile and affected by temperature, whereas PAHs with 5–6 ring are primarily in the particle phase (Ho et al., 2009). In addition, high levels of 4 ring PAHs are associated with coal combustion (Ma et al., 2010); the increasing coal consumption for central heating could lead to increase in the levels of 4 ring PAHs during winter.

Combustion-derived PAHs (COMPAHs, including Flt, Pyr, BaA, Chr, BbF, BkF, BaP, IcdP, and BghiP) can be used to determine the influence of combustion source. As shown in Table 4, the annual average concentrations of COMPAHs were 49 and 64 ng m^{-3} in $PM_{2.5}$ and PM_{10}, respectively, accounting for 83% of Σ_{16}PAHs. The results were comparable with those reported by E'erduosi (42%–84% in $PM_{2.5}$ and 75%–82% in PM_{10}) (Wu et al., 2014). It may be inferred that coal combustion and vehicle emissions are the dominant sources of PAHs in the study area.

3.3 Seasonal variations of n-alkanes

A total of 33 n-alkanes (C_8–C_{40}), pristine (Pr), and phytane (Ph) were measured in this study; C_9 and C_{40} were not detected in the samples. As shown in Table 5, the annual average $\Sigma C_{n\text{-alkanes}}$ concentrations in $PM_{2.5}$ and PM_{10} were 234 and 286 ng m^{-3}, respectively, with the seasonal variation trend of winter (392 ng m^{-3} for $PM_{2.5}$, 476 ng m^{-3} for PM_{10}) > autumn (272 ng m^{-3} for $PM_{2.5}$, 355 ng m^{-3} for PM_{10}) > spring (182 ng m^{-3} for $PM_{2.5}$, 232 ng m^{-3} for PM_{10}) > summer (89 ng m^{-3} for $PM_{2.5}$, 175 ng m^{-3} for PM_{10}). The ratios of $PM_{2.5\text{-n-alkanes}}/PM_{10\text{-n-alkanes}}$ were 0.77, 0.82, 0.78, and 0.51 in autumn, winter, spring, and summer, respectively. This finding suggests that n-alkanes are mainly associated with fine particles except during summer. In addition, both Pr and Ph were detected in all $PM_{2.5}$ and PM_{10} samples. According to Simoneit (1984), Pr and Ph can indicate fossil fuel source. Therefore, it can be concluded that aerosols are generally polluted by fossil fuel. The n-alkane concentrations in this study were within the range of the observed data in Qingdao, North China (258 ng m^{-3} in $PM_{2.5}$) (Guo et al., 2009); higher than those measured in Shanghai (32.2 ng m^{-3} in $PM_{2.5}$) (Cao et al., 2013) and southeastern Tibetan Plateau (1.25 ng m^{-3} in TSP) (Chen et al., 2014); but lower than those measured in Beijing (425.7 ng m^{-3} in $PM_{2.5}$) (Duan et al., 2010).

3.4 Source identification

3.4.1 Diagnostic ratio analysis

Previous studies used diagnostic ratios to identify possible emission sources (Slezakova et al., 2013; Hanedar et al., 2014). In the present study, the ratios of IcdP/(IcdP+BghiP), BaA/(BaA+Chr) and BaP/BghiP were used to identify possible sources of PAHs. IcdP/(IcdP+BghiP) ratio below 0.5 indicates engine fuel combustion, and that higher than 0.5 indicates coal/biomass burning (Yunker et al., 2002). As shown in Table 4, the average values of IcdP/(IcdP+BghiP) ranged from 0.34 to 0.44 in all seasons, implying that PAHs may be influenced by engine fuel combustion. For BaA/(BaA+Chr), ratios below 0.2, 0.20–0.35, and higher than 0.35 indicate petroleum, vehicle emission, and coal combustion sources, respectively (Yunker et al., 2002). In

the present study, the ratios of BaA/(BaA+Chr) were approximately 0.5, indicating the significant contribution of the coal combustion source. BaP/BghiP ratios below 0.60, 0.60–0.90, and higher than 0.90 indicate petroleum, mobile, and coal combustion sources, respectively (Peng et al., 2011). In the present study, the ratios of BaP/BghiP are 0.67 for $PM_{2.5}$ and 0.81 for PM_{10} in winter, indicating that mobile sources are the primary contributors. The ratios of BaP/BghiP are higher than 0.9 in autumn, spring, and summer, reflecting the pollution from coal combustion. Hence, the possible sources of $PM_{2.5\text{-}PAHs}$ and $PM_{10\text{-}PAHs}$ in the study area were coal combustion and vehicle emissions.

Few important indices were used to indicate the potential source for n-alkanes and assess the extent of contribution from biogenic or anthropogenic sources (Cao et al., 2013). Carbon maximum number (C_{max}) was used to indicate the highest concentration of n-alkanes, low C_{max} (i.e., n-$C_{<26}$) indicates that anthropogenic source is dominant, whereas high C_{max} (i.e., n-$C_{>26}$) suggests that more important contributions are from biogenic sources ((i.e., shedding of epicuticular waxes by terrestrial plants) (Abas and Simoneit, 1996; Cecinato et al., 1999). The carbon preference index (CPI, the relative quantities of odd/even carbon number n-alkanes) and the contribution of plant wax (wax%) are commonly used to identify the source of n-alkanes (Simoneit et al., 1991). CPI_1 is defined as the average CPI for the whole range of n-alkanes (C_8–C_{39}), CPI_2 for petrogenic n-alkanes (C_8–C_{25}), and CPI_3 for biogenic n-alkanes (C_{26}–C_{39}). CPI and wax% were calculated as follows:

$$CPI_1 = \Sigma(C_{11} - C_{39})/\Sigma(C_8 - C_{38}), \quad (4)$$

$$CPI_2 = \Sigma(C_{11} - C_{25})/\Sigma(C_8 - C_{24}), \quad (5)$$

$$CPI_3 = \Sigma(C_{27} - C_{39})/\Sigma(C_{26} - C_{38}), \quad (6)$$

$$\%waxC_n = \Sigma(C_n - 0.5(C_{n-1} + C_{n+1}))/\Sigma C_{n\text{-}alkanes} \times 100 \quad (7)$$

In the current study, in both sizes, the C_{max} was C_{29}, followed by C_{25} in autumn; whereas in the other seasons, C_{max} was C_{25}, followed by C_{29} (Fig. 5). This finding reflected that besides anthropogenic emissions, epicuticular wax was also an

important source to the n-alkanes. Table 5 shows the calculated values for CPI_1, CPI_2, CPI_3, and wax% obtained in this study. The annual average CPI values for CPI_1, CPI_2, and CPI_3 n-alkanes in $PM_{2.5}$ and PM_{10} were 1.3, 1.2, and 1.4, respectively. The contribution of plant wax to n-alkane in $PM_{2.5}$ and PM_{10} ranged from 14% to 19%. The results revealed that anthropogenic emissions were the main source of n-alkanes. All the n-alkane indices suggest that the anthropogenic activities were dominant for the contributions of n-alkanes even though some n-alkanes were from terrestrial plants.

3.4.2 PMF analysis

Diagnostic ratios can generally provide qualitative identification for sources of PAHs and n-alkanes. However, further estimation is required to quantify the contribution of the sources. PMF can be used to determine factors of covariant species considering measurement uncertainties (Paatero and Unto, 1994). In the present study, the PMF 5.0 Model was applied. A previous study described the details of PMF analysis (Tao et al., 2014b).

The Pearson correlations between the measured organic species (OC, EC, PAHs and n-alkanes) in PM_{10} and $PM_{2.5}$ samples were estimated to determine whether species of different sizes are formed from similar sources. The results showed good correlations of PAHs in $PM_{2.5}$ with that of PM_{10} ($r = 0.676$) and for n-alkanes ($r = 0.929$) (Table 2). Both this finding and the diagnostic ratios revealed that PAHs and n-alkanes sources of PM_{10} exhibit similar characteristics with those of $PM_{2.5}$. According to the findings from other studies (Shi et al., 2014; Liu et al., 2015), PAHs in PM_{10} and $PM_{2.5}$ were combined into one dataset and introduced into PMF model; in the model, PAHs in PM_{10} and $PM_{2.5}$ were from similar source categories and acquire satisfactory results. In addition, the use of aggregated data in the PMF analysis resulted in improved statistical indicators, such as better Q values and smaller residuals (Moeinaddini et al., 2014). Eventually, 114 samples were inputted into PMF model to identify the main source categories of PAHs and n-alkanes, respectively.

The source profiles of PAHs together with annual contributions of each source are shown in Fig. 6 and seasonal contributions from each source are summarized in Fig. S1, based on their daily simulated values. Four sources were identified from the PMF analysis. The predicted concentration of total PAHs is highly correlated with the observed concentration ($r = 0.996$, $n = 114$). Each of the four factors had a distinctive group of species associated with a specific source class. The contributions of Factor 1 to Σ_{16}PAHs ranged from 9% (winter) to 18% (both in spring and summer), with an annual contribution of 14% (Fig. S1 and Fig. 6). IcdP, BghiP, BbF, BkF, and DaA were the most dominant species, followed by NaP, Chr, and Ace. Indicatory PAHs for industrial boilers and coke oven iron are BbF, IcdP, and BghiP (Kong et al., 2011, 2013). Therefore, Factor 1 represented the pollution of industry. Factor 2 showed the major loading of Flu, Phe, Ant, Flt, Pyr, BaA, and Chr. The profile of Factor 2 was similar to that for residential coal combustion. In addition, Pyr and BaA are regarded as tracers for coal combustion (Wang et al., 2006). Therefore, this factor was classified as coal combustion. The contributions of factor 2 to Σ_{16}PAHs varied from 35% (autumn) to 48% (winter), with an annual contribution of 40% (Fig. S1 and Fig. 6). Coal combustion has the highest contribution to Σ_{16}PAHs in Zhengzhou, which is probably attributable to the coal-dominated energy structure in Zhengzhou. Factor 3 had high loadings of BkF, BbF, IcdP, BaA, Chr, and BghiP, which are typical markers of traffic emissions (Ravindra et al., 2008). Thus, Factor 3 was identified as motor vehicles, and the contributions of this factor to Σ_{16}PAHs ranged from 25% (spring) to 33% (summer), with an annual contribution of 29% (Fig. S1 and Fig. 6). Zhengzhou is an important railway hub of China, which has been experiencing rapid increase in vehicles. Therefore, motor vehicles has become a major contributor to Σ_{16}PAHs in Zhengzhou. Factor 4 mainly loaded with Nap, Acy, Ace, Flu, BaP, and DaA. A similar profile was provided for biomass burning (Simcik et al., 1999), and BaP was a good tracer for biomass burning (Kulkarni and Venkataraman, 2000). Factor 4 was identified as biomass burning, and the contributions of this factor to Σ_{16}PAHs varied

from 13% (summer) to 25% (autumn), with an annual contribution of 17% (Fig. S1 and Fig. 6). The higher contribution of biomass burning in autumn is probably attributable to the increasing of open burning of straws during harvest season.

The n-alkanes ranged from C_{12} to C_{38}, Pr and Ph were selected to run PMF. Finally, three n-alkane source factors were identified. The predicted concentration of total n-alkanes was highly correlated with the observed concentration ($r = 0.994$, $n = 114$). Factor 1 could be attributed to the fossil fuel source mainly from vehicle emission and coal combustion because it had strongly correlation with low and medium molecular weight n-alkanes (< C_{27}), Pr and Ph (Fig. 7). Schauer et al. (1999, 2002) concluded that n-alkanes (C_{20}–C_{27}) were produced from the combustion of gasoline, and C_{12}–C_{20} from the combustion of diesel. The high factor loadings for Pr and Ph indicate petroleum fuel (Simoneit, 1984; Schauer et al., 2002). The contributions of this factor to total n-alkanes ranged from 44% (summer) to 54% (winter), with an annual contribution of 48% (Fig. S2 and Fig. 7). The results reflected that vehicle emission and coal combustion were the main sources of n-alkanes in Zhengzhou. Factor 2 with C_{25}–C_{38}; however, no factor loadings were observed for Pr and Ph (Fig. 7), indicating that the contribution from biogenic sources were derived from plant waxes (Guo et al., 2009). The contributions of this factor to total n-alkanes ranged from 14% (winter) to 25% (summer), with an annual contribution of 18% (Fig. S2 and Fig. 7). The contributions of biogenic source were larger in summer and autumn (22%) may due to the mechanical abrasion of higher plant waxes, vegetation debris and soil erosion (Guo et al., 2009). Factor 3 was characterized by low molecular weight n-alkanes (C_{12}–C_{16}) and long-chain n-alkanes (C_{27}–C_{38}), as well as Pr and Ph (Fig. 7), indicating the contribution of fossil fuel and biogenic sources. The contributions of this factor to total n-alkanes varied from 31% (both in autumn and summer) to 35% (spring), with an annual contribution of 34% (Fig. S2 and Fig. 7).

Good agreement with the PMF model and diagnostic ratios indicated that coal

combustion and vehicle emission were the major pollution sources of PAHs and n-alkanes in urban Zhengzhou. Though there were minor differences in the source contributions during the four seasons, the main pollution sources were consistent. This finding was consistent with the fact that coal is the main energy source in Zhengzhou, especially in heating season. In addition, according to Henan Statistical Yearbook of 2012–2015, the vehicle population in Zhengzhou increased from 1.24 million in 2011 to 2.92 million in 2014. The increasing private vehicle ownership aggravated the air pollution in recent years.

4. Conclusions

In this study, $PM_{2.5}$ and PM_{10} samples were simultaneously collected to investigate the concentration, seasonal variation, and possible sources of carbonaceous species from October 2014 to July 2015 in Zhengzhou, a core city of CPER. The annual average concentrations of $PM_{2.5}$ and PM_{10} were 146 and 214 μg m^{-3}, which were 4-fold and 3-fold of National Ambient Air Quality Standard of China ($PM_{2.5}$: 35 μg m^{-3}, PM_{10}: 70 μg m^{-3}), respectively, reflecting the severe PM pollution in the study area.

The concentrations of these carbonaceous components showed distinct seasonal variation with winter > autumn > spring > summer in $PM_{2.5}$ and PM_{10}. TCA accounted for 32% and 30% of $PM_{2.5}$ and PM_{10}, revealing that carbonaceous aerosol was an important component in PM. The annual average concentration of Σ_{16}PAHs in $PM_{2.5}$ and PM_{10} were 58 ng m^{-3} and 78 ng m^{-3}, and were 234 ng m^{-3} and 286 ng m^{-3} for n-alkanes. Σ_{16}PAHs and Σn-alkane concentrations were at high levels compared with those reported in other cities. All concentration data revealed that the main portion of organic components was adsorbed onto the fine particulate. Additionally, BaP concentration (3.3 ng m^{-3} in $PM_{2.5}$, 5.6 ng m^{-3} in PM_{10}) exceeded air quality standard (1 ng m^{-3}) in China, suggesting a potential health risk.

Based on the significant correlations of PAHs and n-alkanes in PM_{10} and $PM_{2.5}$ and diagnostic ratios results, PAHs and n-alkanes in PM_{10} and $PM_{2.5}$ have similar

source categories. PMF results indicated that PAHs could be attributed to industry (14%), coal (40%), motor vehicles (29%), and biomass burning (17%); n-alkanes were mainly derived from fossil fuel burning (48%), biogenic (18%), and combination of fossil fuel and biogenic sources (34%). Coal combustion and motor vehicles emission were the most important sources. These results can provide useful guidance for further air quality improvement.

Acknowledgments

This study is supported by Ministry of Environmental Protection of the People's Republic of China (grant no. 201409010). Authors would like to appreciate those assisting in analyses: Junhua Wei, Shenbo Wang, Shijie Yu, Qiang Li, Xue Yu.

References:

Abas, M.R.B., Simoneit, B.R.T., 1996. Composition of extractable organic matter of air particles from malaysia: Initial study. Atmos. Environ. 30, 2779-2793.

Akyüz, M., Çabuk, H., 2009. Meteorological variations of $PM_{2.5}/PM_{10}$ concentrations and particle-associated polycyclic aromatic hydrocarbons in the atmospheric environment of Zonguldak, Turkey. J. Hazard. Mater. 170, 13-21.

Bi, X., Sheng, G., Peng, A.P., Zhang, Z., Fu, J., 2002. Extractable organic matter in PM_{10} from LiWan district of Guangzhou City, PR China. Sci. Total Environ. 300, 213-228.

Bi, X., Sheng, G., Peng, P.A., Chen, Y., Zhang, Z., Fu, J., 2003. Distribution of particulate- and vapor-phase n-alkanes and polycyclic aromatic hydrocarbons in urban atmosphere of Guangzhou, China. Atmos. Environ. 37, 289-298.

Birch, M.E., Cary, R.A., 1996. Elemental carbon-Based method for monitoring occupational exposures to particulate diesel exhaust. Aerosol Sci. Technol. 25, 221-241.

Callén, M.S., Iturmendi, A., López, J.M., 2014. Source apportionment of atmospheric $PM_{2.5\text{-bound}}$ polycyclic aromatic hydrocarbons by a PMF receptor model. Assessment of potential risk for human health. Environ. Pollut. 195, 167-177.

Cao, J.J., Lee, S.C., Chow, J.C., Watson, J.G., Ho, K.F., Zhang, R.J., Jin, Z.D., Shen, Z.X., Chen, G.C., Kang, Y.M., 2007. Spatial and seasonal distributions of carbonaceous aerosols over China. J. Geophys. Res. Atmos. D112, 11-22.

Cao, J.J., Zhu, C.S., Tie, X.X., Geng, F.H., Xu, H.M., Ho, S.S.H., Wang, G.H., Han, Y.M., Ho, K.F.,

2013. Characteristics and sources of carbonaceous aerosols from Shanghai, China. Atmos. Chem. Phys. 13, 803-817.

Castro, L.M., Pio, C.A., Harrison, R.M., Smith, D.J.T., 1999. Carbonaceous aerosol in urban and rural European atmospheres: estimation of secondary organic carbon concentrations. Atmos. Environ. 33, 2771-2781.

Cecinato, A., Marino, F., Di Filippo, P., Lepore, L., Possanzini, M., 1999. Distribution of n-alkanes, polynuclear aromatic hydrocarbons and nitrated polynuclear aromatic hydrocarbons between the fine and coarse fractions of inhalable atmospheric particulates. J. Chromatogr. A 846, 255-264.

Chan, Y., Hawas, O., Hawker, D., Vowles, P., Cohen, D.D., Stelcer, E., Simpson, R., Golding, G., Christensen, E., 2011. Using multiple type composition data and wind data in PMF analysis to apportion and locate sources of air pollutants. Atmos. Environ. 45, 439-449.

Chen, D., Cui, H., Zhao, Y., Yin, L., Lu, Y., Wang, Q., 2017. A two-year study of carbonaceous aerosols in ambient $PM_{2.5}$ at a regional background site for western Yangtze River Delta, China. Atmos. Res. 183, 351-361.

Chen, Y., Zhi, G., Feng, Y., Fu, J., Feng, J., Sheng, G., Simoneit, B.R.T., 2006. Measurements of emission factors for primary carbonaceous particles from residential raw-coal combustion in China. Geophys. Res. Lett. 332, 382-385.

Chen, Y., Cao, J., Zhao, J., Xu, H., Arimoto, R., Wang, G., Han, Y., Shen, Z., Li, G., 2014. n-Alkanes and polycyclic aromatic hydrocarbons in total suspended particulates from the southeastern Tibetan Plateau: Concentrations, seasonal variations, and sources. Sci. Total Environ. 470-471, 9-18.

Chow, J.C., Watson, J.G., Lu, Z., Lowenthal, D.H., Frazier, C.A., Solomon, P.A., Thuillier, R.H., Magliano, K., 1996. Descriptive analysis of $PM_{2.5}$ and PM_{10} at regionally representative locations during SJVAQS/AUSPEX. Atmos. Environ. 30, 2079-2112.

Duan, F., He, K., Liu, X., 2010. Characteristics and source identification of fine particulate n-alkanes in Beijing, China. J. Environ. Sci. 22, 998-1005.

Duan, J., Tan, J., Cheng, D., Bi, X., Deng, W., Sheng, G., Fu, J., Wong, M.H., 2007. Sources and characteristics of carbonaceous aerosol in two largest cities in Pearl River Delta Region, China. Atmos. Environ. 41, 2895-2903.

Duarte, R.M.B.O., Mieiro, C.L., Penetra, A., Pio, C.A., Duarte, A.C., 2008. Carbonaceous materials in size-segregated atmospheric aerosols from urban and coastal-rural areas at the Western European Coast. Atmos. Res. 90, 253-263.

Gao, B., Guo, H., Wang, X., Zhao, X., Ling, Z., Zhang, Z., Liu, T., 2012. Polycyclic aromatic hydrocarbons in $PM_{2.5}$ in Guangzhou, southern China: Spatiotemporal patterns and emission sources. J. Hazard. Mater. 239, 78-87.

Geng, N., Wang, J., Xu, Y., Zhang, W., Chen, C., Zhang, R., 2013. $PM_{2.5}$ in an industrial district of Zhengzhou, China: Chemical composition and source apportionment. Particuology 11, 99-109.

Gray, H.A., Cass, G.R., Huntzicker, J.J., Heyerdahl, E.K., Rau, J.A., 1986. Characteristics of atmospheric organic and elemental carbon particle concentrations in Los Angeles. Environ. Sci. Technol. 20, 580-589.

Guo, Z., Lin, T., Zhang, G., Hu, L., Zheng, M., 2009. Occurrence and sources of polycyclic aromatic hydrocarbons and n-alkanes in $PM_{2.5}$ in the roadside environment of a major city in China. J. Hazard. Mater. 170, 888-894.

Hanedar, A., Alp, K., Kaynak, B., Avşar, E., 2014. Toxicity evaluation and source apportionment of Polycyclic Aromatic Hydrocarbons (PAHs) at three stations in Istanbul, Turkey. Sci. Total Environ. 488-489, 437-446.

He, J., Fan, S., Meng, Q., Sun, Y., Zhang, J., Zu, F., 2014. Polycyclic aromatic hydrocarbons (PAHs) associated with fine particulate matters in Nanjing, China: Distributions, sources and meteorological influences. Atmos. Environ. 89, 207-215.

Ho, K.F., Ho, S.S.H., Lee, S.C., Cheng, Y., Chow, J.C., Watson, J.G., Louie, P.K.K., Tian, L., 2009. Emissions of gas- and particle-phase polycyclic aromatic hydrocarbons (PAHs) in the Shing Mun Tunnel, Hong Kong. Atmos. Environ. 43, 6343-6351.

Huang, R., Zhang, Y., Bozzetti, C., Ho, K., Cao, J., Han, Y., Daellenbach, K.R., Slowik, J.G., Platt, S.M., Canonaco, F., Zotter, P., Wolf, R., Pieber, S.M., Bruns, E.A., Crippa, M., Ciarelli, G., Piazzalunga, A., Schwikowski, M., Abbaszade, G., Schnelle-Kreis, J., Zimmermann, R., An, Z., Szidat, S., Baltensperger, U., Haddad, I.E., Prévôt, A.S.H., 2014. High secondary aerosol contribution to particulate pollution during haze events in China. Nature 514, 218-222.

Jacobson, M.Z., 2001. Strong radiative heating due to the mixing state of black carbon in atmospheric aerosols. Nature 409, 695-697.

Jang, E., Alam, M.S., Harrison, R.M., 2013. Source apportionment of polycyclic aromatic hydrocarbons in urban air using positive matrix factorization and spatial distribution analysis. Atmos. Environ. 79, 271-285.

Kong, S., Ji, Y., Li, Z., Lu, B., Bai, Z., 2013. Emission and profile characteristic of polycyclic aromatic hydrocarbons in $PM_{2.5}$ and PM_{10} from stationary sources based on dilution sampling. Atmos. Environ.

77, 155-165.

Kong, S., Shi, J., Lu, B., Qiu, W., Zhang, B., Peng, Y., Zhang, B., Bai, Z., 2011. Characterization of PAHs within PM_{10} fraction for ashes from coke production, iron smelt, heating station and power plant stacks in Liaoning Province, China. Atmos. Environ. 45, 3777-3785.

Kulkarni, P., Venkataraman, C., 2000. Atmospheric polycyclic aromatic hydrocarbons in Mumbai, India. Atmos. Environ. 34, 2785-2790.

Li, B., Zhang, J., Zhao, Y., Yuan, S., Zhao, Q., Shen, G., Wu, H., 2015. Seasonal variation of urban carbonaceous aerosols in a typical city Nanjing in Yangtze River Delta, China. Atmos. Environ. 106, 223-231.

Liu, G., Peng, X., Wang, R., Tian, Y., Shi, G., Wu, J., Zhang, P., Zhou, L., Feng, Y., 2015. A new receptor model-incremental lifetime cancer risk method to quantify the carcinogenic risks associated with sources of particle-bound polycyclic aromatic hydrocarbons from Chengdu in China. J. Hazard. Mater. 283, 462-468.

Ma, W., Li, Y., Qi, H., Sun, D., Liu, L., Wang, D., 2010. Seasonal variations of sources of polycyclic aromatic hydrocarbons (PAHs) to a northeastern urban city, China. Chemosphere 79, 441-447.

Moeinaddini, M., Esmaili Sari, A., Riyahi Bakhtiari, A., Chan, A.Y., Taghavi, S.M., Hawker, D., Connell, D., 2014. Source apportionment of PAHs and n-alkanes in respirable particles in Tehran, Iran by wind sector and vertical profile. Environ. Sci. Pollut. Res. 21, 7757-7772.

Nisbet, C., LaGoy, P., 1992. Toxic equivalency factors (TEFs) for polycyclic aromatic hydrocarbons (PAHs). Regul. Toxicol. Pharmacol. 16, 290-300.

Okuda, T., Okamoto, K., Tanaka, S., Shen, Z., Han, Y., Huo, Z., 2010. Measurement and source identification of polycyclic aromatic hydrocarbons (PAHs) in the aerosol in Xi'an, China, by using automated column chromatography and applying positive matrix factorization (PMF). Sci. Total Environ. 408, 1909-1914.

Paatero, P., Unto, T., 1994. Positive matrix factorization: A non-negative factor model with optimal utilization of error estimates of data values. Environmetrics 5, 111-126.

Paatero, P., Hopke, P.K., 2003. Discarding or downweighting high noise variables in factor analytic models. Anal. Chim. Acta 490 (1), 277–289.

Pachauri, T., Singla, V., Satsangi, A., Lakhani, A., Kumari, K.M., 2013. Characterization of carbonaceous aerosols with special reference to episodic events at Agra, India. Atmos. Res. 128, 98-110.

Paraskevopoulou, D., Liakakou, E., Gerasopoulos, E., Mihalopoulos, N., 2015. Sources of atmospheric aerosol from long-term measurements (5 years) of chemical composition in Athens, Greece. Sci. Total Environ. 527, 165-178.

Peng, C., Chen, W., Liao, X., Wang, M., Ouyang, Z., Jiao, W., Bai, Y., 2011. Polycyclic aromatic hydrocarbons in urban soils of Beijing: Status, sources, distribution and potential risk. Environ. Pollut. 159, 802-808.

Pipal, A.S., Gursumeeran Satsangi, P., 2015. Study of carbonaceous species, morphology and sources of fine ($PM_{2.5}$) and coarse (PM_{10}) particles along with their climatic nature in India. Atmos. Res. 154, 103-115.

Rajput, P., Sarin, M.M., Rengarajan, R., Singh, D., 2011. Atmospheric polycyclic aromatic hydrocarbons (PAHs) from post-harvest biomass burning emissions in the Indo-Gangetic Plain: Isomer ratios and temporal trends. Atmos. Environ. 45, 6732-6740.

Ravindra, K, Sokhi, R, Van Grieken, R., 2008. Atmospheric polycyclic aromatic hydrocarbons: Source attribution, emission factors and regulation. Atmos. Environ. 42, 2895-2921.

Satsangi, A., Pachauri, T., Singla, V., Lakhani, A., Kumari, K.M., 2012. Organic and elemental carbon aerosols at a suburban site. Atmos. Res. 113, 13-21.

Schauer, J.J., Kleeman, M.J., Cass, G.R., Simoneit, B.R., 1999. Measurement of emissions from air pollution sources. 2. C_1 through C_{30} organic compounds from medium duty diesel trucks. Environ. Sci. Technol. 33, 1578-1587.

Schauer, J.J., Kleeman, M.J., Cass, G.R., Simoneit, B.R., 2002. Measurement of emissions from air pollution sources. 5. C_1-C_{32} organic compounds from gasoline-powered motor vehicles. Environ. Sci. Technol. 36, 1169-1180.

Shen, G., Wang, W., Yang, Y., Chen, Z., Min, Y., Xue, M., Ding, J., Li, W., Wang, B., Shen, H., 2010. Emission factors and particulate matter size distribution of polycyclic aromatic hydrocarbons from residential coal combustions in rural Northern China. Atmos. Environ. 44, 5237-5243.

Shi, G., Liu, G., Tian, Y., Zhou, X., Peng, X., Feng, Y., 2014. Chemical characteristic and toxicity assessment of particle associated PAHs for the short-term anthropogenic activity event: During the Chinese New Year's Festival in 2013. Sci. Total Environ. 482-483, 8-14.

Shi, G., Zhou, X., Jiang, S., Tian, Y., Liu, G., Feng, Y., Chen, G., Liang, Y., 2015. Further insights into the composition, source, and toxicity of PAHs in size-resolved particulate matter in a megacity in China. Environ. Toxicol. Chem. 34, 480-487.

Simcik, M.F., Eisenreich, S.J., Lioy, P.J., 1999. Source apportionment and source/sink relationships of PAHs in the coastal atmosphere of Chicago and Lake Michigan. Atmos. Environ. 33, 5071-5079.

Simoneit, B.R.T., 1984. Organic matter of the troposphere−III. Characterization and sources of petroleum and pyrogenic residues in aerosols over the western united states. Atmos. Environ. 18, 51-67.

Simoneit, B.R.T., Cardoso, J.N., Robinson, N., 1991. An assessment of terrestrial higher molecular weight lipid compounds in aerosol particulate matter over the south atlantic from about 30−70°S. Chemosphere 23, 447-465.

Slezakova, K., Castro, D., Delerue Matos, C., Alvim Ferraz, M.D.C., Morais, S., Pereira, M.D.C., 2013. Impact of vehicular traffic emissions on particulate-bound PAHs: Levels and associated health risks. Atmos. Res. 127, 141-147.

Tao, M., Chen, L., Xiong, X., Zhang, M., Ma, P., Tao, J., Wang, Z., 2014a. Formation process of the widespread extreme haze pollution over northern China in January 2013: Implications for regional air quality and climate. Atmos. Environ. 98, 417-425.

Tao, J., Gao, J., Zhang, L., Zhang, R., Che, H., Zhang, Z., Lin, Z., Jing, J., Cao, J., Hsu, S.C., 2014b. $PM_{2.5}$ pollution in a megacity of southwest China: source apportionment and implication. Atmos. Chem. Phys. 14, 8679-8699.

Turpin, B.J., Huntzicker, J.J., 1991. Secondary formation of organic aerosol in the Los Angeles basin: A descriptive analysis of organic and elemental carbon concentrations. Atmos. Environ. Part A. General Topics Gen. Top. 25, 207-215.

Turpin, B.J., Lim, H., 2001. Species contributions to $PM_{2.5}$ mass concentrations: revisiting common assumptions for estimating organic mass. Aerosol Sci. Technol. 35, 602-610.

USEPA, 2014. Positive Matrix Factorization (PMF) 5.0 Fundamentals & User Guide. Office of Research and Development.

Wang, G., Cheng, S., Li, J., Lang, J., Wen, W., Yang, X., Tian, L., 2015a. Source apportionment and seasonal variation of $PM_{2.5}$ carbonaceous aerosol in the Beijing-Tianjin-Hebei Region of China. Environ. Monit. Assess. 187, 1-13.

Wang, G., Huang, L., Zhao, X., Niu, H., Dai, Z., 2006. Aliphatic and polycyclic aromatic hydrocarbons of atmospheric aerosols in five locations of Nanjing urban area, China. Atmos. Res. 81, 54-66.

Wang, J., Geng, N.B., Xu, Y.F., Zhang, W.D., Tang, X.Y., Zhang, R.Q., 2014. PAHs in $PM_{2.5}$ in

Zhengzhou: concentration, carcinogenic risk analysis, and source apportionment. Environ. Monit. Assess. 186, 7461-7473.

Wang, J., Li, X., Jiang, N., Zhang, W., Zhang, R., Tang, X., 2015b. Long term observations of $PM_{2.5}$-associated PAHs: Comparisons between normal and episode days. Atmos. Environ. 104, 228-236.

WHO (2000). Polynuclear aromatic hydrocarbons. In: Air quality guidelines for Europe, second edition. (Chapter 5.9). World Health Organization, Geneva.

Wu, D., Wang, Z., Chen, J., Kong, S., Fu, X., Deng, H., Shao, G., Wu, G., 2014. Polycyclic aromatic hydrocarbons (PAHs) in atmospheric $PM_{2.5}$ and PM_{10} at a coal-based industrial city: Implication for PAH control at industrial agglomeration regions, China. Atmos. Res. 149, 217-229.

Yunker, M.B., Macdonald, R.W., Vingarzan, R., Mitchell, R.H., Goyette, D., Sylvestre, S., 2002. PAHs in the Fraser River basin: A critical appraisal of PAH ratios as indicators of PAH source and composition. Org. Geochem. 33, 489-515.

Zhang, Y., Schauer, J.J., Zhang, Y., Zeng, L., Wei, Y., Liu, Y., Shao, M., 2008. Characteristics of particulate carbon emissions from real-world Chinese coal combustion. Environ. Sci. Technol. 42, 5068-5073.

Zhang, Y., Sheesley, R.J., Schauer, J.J., Lewandowski, M., Jaoui, M., Offenberg, J.H., Kleindienst, T.E., Edney, E.O., 2009. Source apportionment of primary and secondary organic aerosols using positive matrix factorization (PMF) of molecular markers. Atmos. Environ. 43, 5567-5574.

Zhang, Y.X., Shao, M., Zhang, Y.H., Zeng, L.M., Ling-Yan, H.E., Zhu, B., Wei, Y.J., Zhu, X.L., 2007. Source profiles of particulate organic matters emitted from cereal straw burnings. J. Environ. Sci. 19, 167-175.

Zhao, P., Dong, F., Yang, Y., He, D., Zhao, X., Zhang, W., Yao, Q., Liu, H., 2013. Characteristics of carbonaceous aerosol in the region of Beijing, Tianjin, and Hebei, China. Atmos. Environ. 71, 389-398.

Zhou, H., He, J., Zhao, B., Zhang, L., Fan, Q., Lü, C., Dudagula, Liu, T., Yuan, Y., 2016. The distribution of PM_{10} and $PM_{2.5}$ carbonaceous aerosol in Baotou, China. Atmos. Res. 178-179, 102-113.

Zhou, J., Xing, Z., Deng, J., Du, K., 2016. Characterizing and sourcing ambient $PM_{2.5}$ over key emission regions in China I: Water-soluble ions and carbonaceous fractions. Atmos. Environ. 135, 20-30.

Table 1 Seasonal meteorological data for Zhengzhou during sample period

	autumn		winter		spring		summer	
	average	range	average	range	average	range	average	range
Wind speed ($m \cdot s^{-1}$)	2.2 ± 4.3	0.8-5.8	2.1 ± 3.1	1.4-3.9	2.7 ± 3.2	1.4-3.9	1.7 ± 1.7	1.4-2.8
Relative humidity (%)	60 ± 15	34-83	47 ± 19	17-79	55 ± 15	29-80	67 ± 10	53-85
Pressure (hPa)	1021 ± 4	1014-1028	1026 ± 6	1014-1035	1017 ± 8	1005-1031	1006 ± 4	999-1012
Temperature (°C)	17.4 ± 1.8	14-20	5.1 ± 4.3	1-16	12.9 ± 3.7	8-21	26.4 ± 2.3	22-31

Table 2 Concentration of PM mass, OC and EC in Zhengzhou during sampling period (μg m^{-3})

Species	Autumn		Winter		Spring		Summer		Annual average	
	$PM_{2.5}$ (n=15)	PM_{10} (n=15)	$PM_{2.5}$ (n=16)	PM_{10} (n=8)	$PM_{2.5}$ (n=14)	PM_{10} (n=14)	$PM_{2.5}$ (n=16)	PM_{10} (n=16)	$PM_{2.5}$ (n=61)	PM_{10} (n=53)
PM mass	154 ± 41	252 ± 71	179 ± 90	263 ± 73	147 ± 31	202 ± 47	102 ± 22	164 ± 42	146 ± 59	214 ± 68
OC	25 ± 21	37 ± 27	45 ± 32	59 ± 31	22 ± 9	28 ± 12	12 ± 4	22 ± 11	27 ± 27	34 ± 23
EC	5 ± 2	7 ± 2	17 ± 9	30 ± 18	8 ± 3	11 ± 4	7 ± 2	12 ± 5	11 ± 13	13 ± 11
SOC	14 ± 22	20 ± 27	21 ± 22	23 ± 11	10 ± 8	13 ± 11	5 ± 3	10 ± 4	12 ± 16	19 ± 17
TCA	45 ± 33	67 ± 44	99 ± 86.5	125± 66	44 ± 16	56 ± 22	27 ± 8	46 ± 22	51 ± 43	67 ± 45
OC/EC	5.1±2.2	5.3±1.8	2. 5 ± 0.8	2. 0 ± 0.3	2.7 ± 1.2	2. 7 ± 1. 3	1.9 ± 0.4	2.2 ± 0.3	3.0 ± 2.9	3.2 ± 2.7
SOC/OC	0.44 ± 0.19	0.42 ± 0.18	0.37 ± 0.08	0.39 ± 0.08	0.36 ± 0.17	0.39 ± 0.19	0.32 ± 0.09	0.22 ± 0.08	0.38 ± 0.16	0.30 ± 0.19
TCA/PM	0.27 ± 0.10	0.25 ± 0.09	0.47 ± 0.17	0.50 ± 0.13	0.29 ± 0.08	0.28 ± 0.09	0.26 ± 0.07	0.28 ± 0.08	0.32 ± 0.14	0.30 ± 0.11

Table 3 Pearson correlation coefficients for organic compounds between PM_{10} and $PM_{2.5}$

		PM_{10}					$PM_{2.5}$				
		PM_{10}	OC	EC	n-alkanes	PAHs	$PM_{2.5}$	OC	EC	n-alkanes	PAHs
PM_{10}	PM_{10}	1	.800**	.473**	.722**	.566**	**.888****	.711**	.489**	.716**	.395**
	OC		1	.674**	.837**	.591**	.828**	**.872****	.663**	.782**	.246
	EC			1	.678**	.741**	.545**	.346*	**.932****	.661**	.228
	n-alkanes				1	.782**	.717**	.646**	.635**	**.929****	.453**
	PAHs					1	.509**	.368**	.685**	.724**	**.676****
$PM_{2.5}$	$PM_{2.5}$						1	.781**	.574**	.762**	.175
	OC							1	.400**	.585**	.193
	EC								1	.658**	.207
	n-alkanes									1	.396**
	PAHs										1

* The correlation coefficient was significant at the 0.05 level (both sides).

** The correlation coefficient was significant at the 0.01 level (both sides).

Table 4 Total concentration and molecular diagnostic parameters of PAHs in $PM_{2.5}$ and PM_{10}

species	Autumn		Winter		Spring		Summer		Annual average	
	$PM_{2.5}$ (n=15)	PM_{10} (n=15)	$PM_{2.5}$ (n=16)	PM_{10} (n=8)	$PM_{2.5}$ (n=15)	PM_{10} (n=15)	$PM_{2.5}$ (n=16)	PM_{10} (n=16)	$PM_{2.5}$ (n=62)	PM_{10} (n=54)
Σ_{16}PAHs (ng m^{-3})	57 ± 17	86 ± 25	114 ± 76	181 ± 78	37 ± 19	58 ± 23	23 ± 14	36± 22	58 ± 54	78 ± 60
CANPAHs (ng m^{-3})	37 ± 12	53 ± 15	54 ± 40	95 ± 55	25 ± 14	38 ± 16	17 ± 12	27 ± 18	34 ± 26	48 ± 34
CANPAHs/Σ_{16}PAHs	0.65	0.62	0.47	0.52	0.66	0.66	0.73	0.75	0.59	0.62
COMPAHs (ng m^{-3})	48 ± 16	70 ± 21	90 ± 63	145 ± 68	32 ±17	50 ± 20	20 ± 13	32 ±20	49 ± 43	64 ± 48
COMPAHs/Σ_{16}PAHs	0.84	0.81	0.79	0.80	0.86	0.84	0.87	0.88	0.83	0.83
$\Sigma_{16}PAHs_{TEQ}$ (ng m^{-3})	7 ± 3	11 ± 4	8 ± 4	16 ± 7	5 ± 3	8 ± 3	4 ± 2	6 ± 4	6 ± 3	9 ± 6
IcdP/(IcdP+BghiP)	0.40	0.43	0.44	0.39	0.34	0.35	0.37	0.38	0.39	0.39
BaA/(BaA+Chr)	0.49	0.51	0.50	0.51	0.50	0.52	0.50	0.50	0.50	0.51
BaP/BghiP	0.91	1.14	0.67	0.81	1.29	1.20	0.95	1.14	0.92	1.09

Table 5 Total concentration and molecular diagnostic parameters of n-alkanes in $PM_{2.5}$ and PM_{10} ($ng\ m^{-3}$)

	Autumn		Winter		Spring		Summer		Annual average	
species	$PM_{2.5}$ (n = 15)	PM_{10} (n = 15)	$PM_{2.5}$ (n = 16)	PM_{10} (n = 8)	$PM_{2.5}$ (n = 15)	PM_{10} (n = 15)	$PM_{2.5}$ (n = 16)	PM_{10} (n = 16)	$PM_{2.5}$ (n = 62)	PM_{10} (n = 54)
$\Sigma C_{n\text{-alkanes}}$ ($ng\ m^{-3}$)	272 ± 78	355± 86	392 ± 203	476 ± 204	182 ± 58	232 ± 65	89 ± 24	175 ± 63	234 ± 160	286 ± 146
CPI_1 [a]	1.3	1.3	1.2	1.2	1.3	1.2	1.3	1.3	1.3	1.3
CPI_2 [b]	1.1	1.2	1.5	1.4	1.1	1.1	1.0	1.1	1.2	1.2
CPI_3 [c]	1.6	1.5	1.2	1.3	1.4	1.3	1.3	1.4	1.4	1.4
Wax% [d]	19	18	16	14	17	15	18	15	17± 6	16 ± 7
C_{max}	C_{29}	C_{29}	C_{25}	C_{25}	C_{25}	C_{25}	C_{25}	C_{25}	C_{25}	C_{25}

[a] total n-alkanes: $CPI_1 = \Sigma(C_{11} - C_{39})/\Sigma(C_8 - C_{38})$

[b] petrogenic n-alkanes: $CPI_2 = \Sigma(C_{11} - C_{25})/\Sigma(C_8 - C_{24})$

[c] biogenic n-alkanes: $CPI_3 = \Sigma(C_{27} - C_{39})/\Sigma(C_{26} - C_{38})$

[d] $\%waxC_n = \Sigma(C_n - 0.5(C_{n-1} + C_{n+1}))/\Sigma C_{n\text{-alkanes}} \times 100$ (Simoneit et al., 1991).

Figure captions:

Fig. 1. Location of the sampling site

Fig. 2. Daily concentration of $PM_{2.5}$, PM_{10}, EC, and OC during the sampling period

Fig. 3. Seasonal variation of 16 PAHs in $PM_{2.5}$ and PM_{10}

Fig. 4. Percentages of PAHs in $PM_{2.5}$ and PM_{10} in Zhengzhou

Fig. 5. Seasonal distribution of n-alkanes in $PM_{2.5}$ and PM_{10}

Fig. 6. (a) PAHs source profiles and (b) source contributions derived from PMF

Fig. 7. (a) n-Alkanes source profiles and (b) source contributions derived from PMF

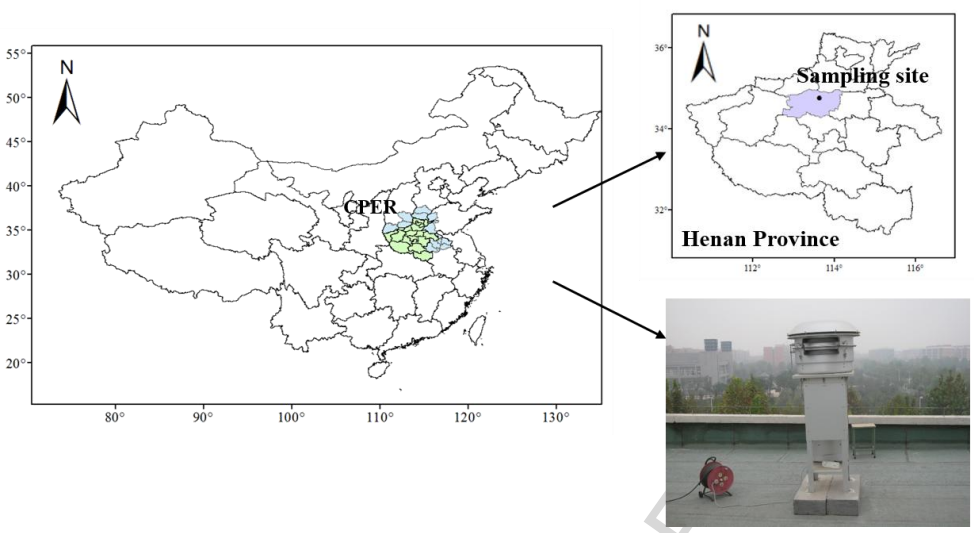

Fig. 1. Location of the sampling site

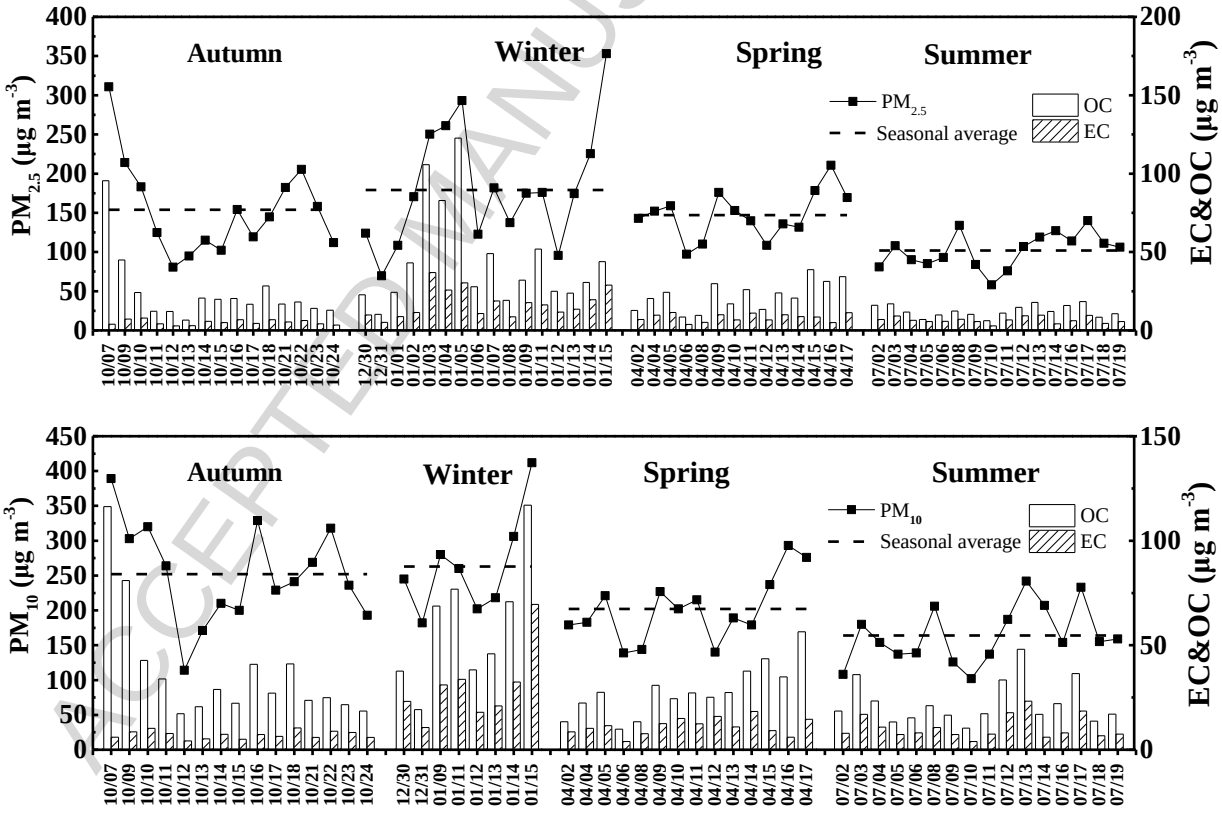

Fig. 2. Daily concentration of $PM_{2.5}$, PM_{10}, EC, and OC during the sampling period

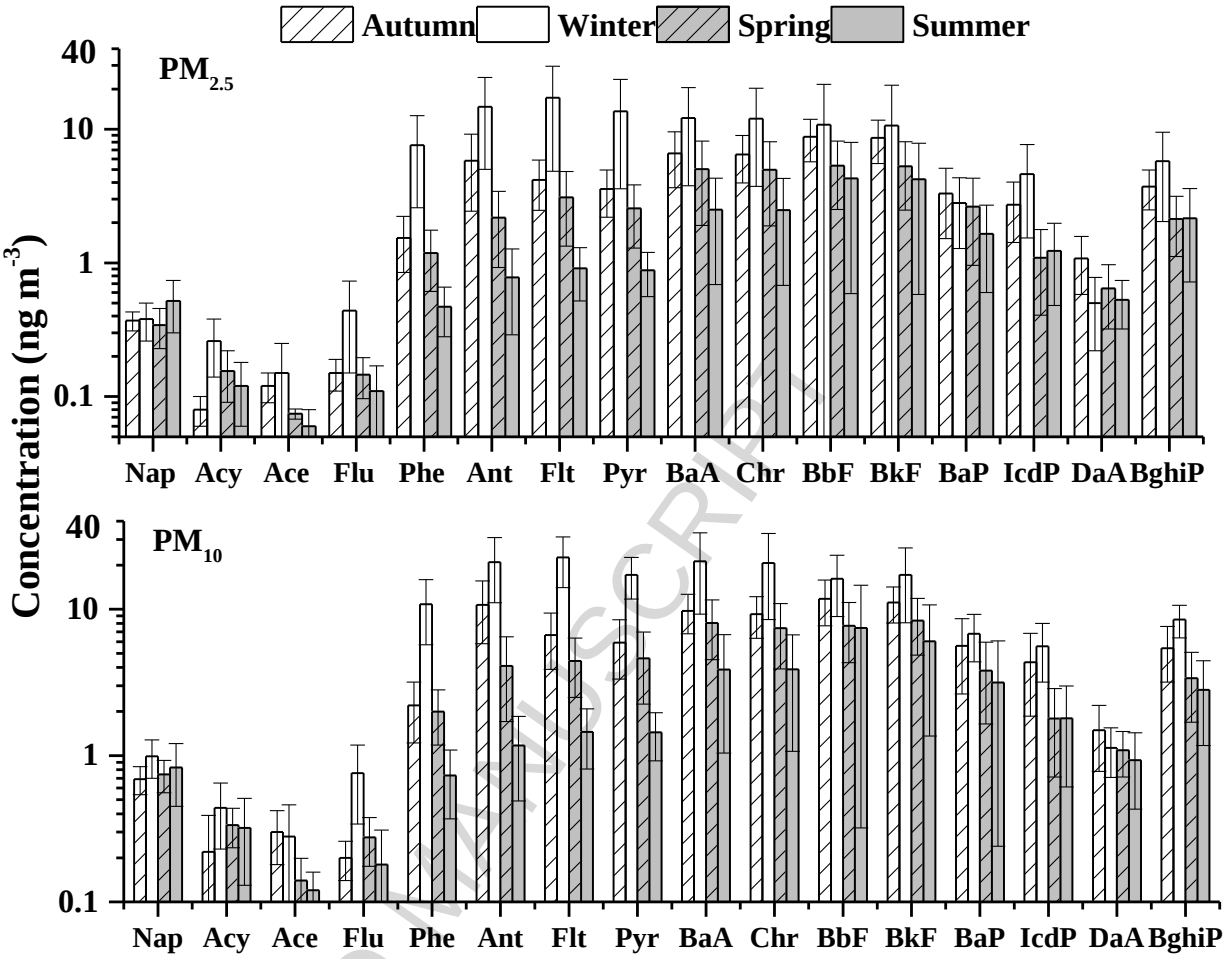

Fig. 3. Seasonal variation of 16 PAHs in $PM_{2.5}$ and PM_{10}

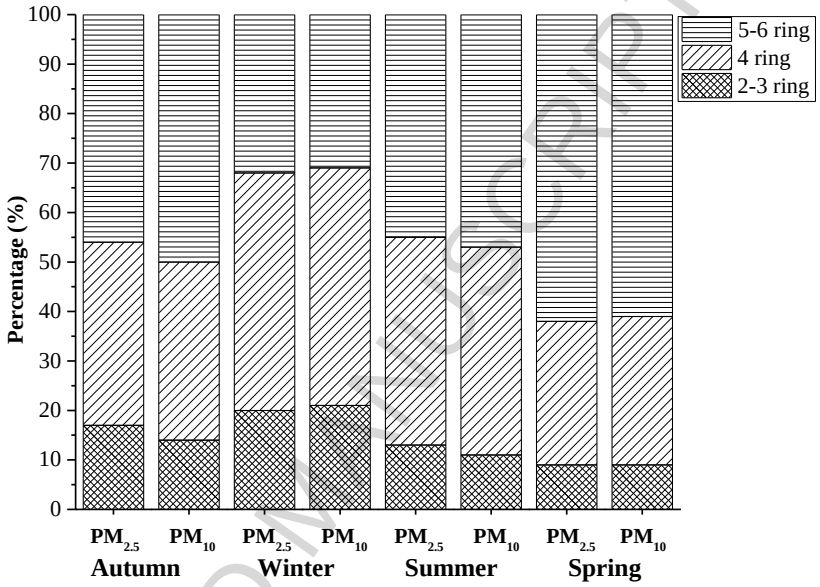

Fig. 4. Percentages of PAHs in $PM_{2.5}$ and PM_{10} in Zhengzhou

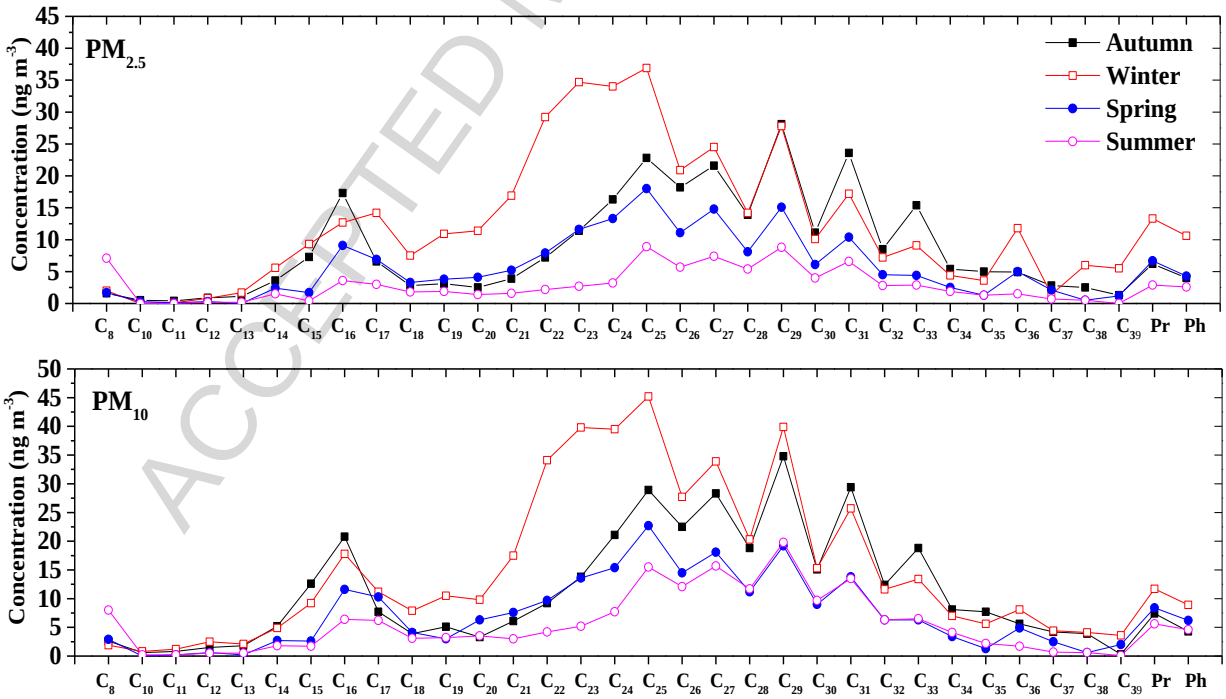

Fig. 5. Seasonal distribution of n-alkanes in PM_{10} and $PM_{2.5}$

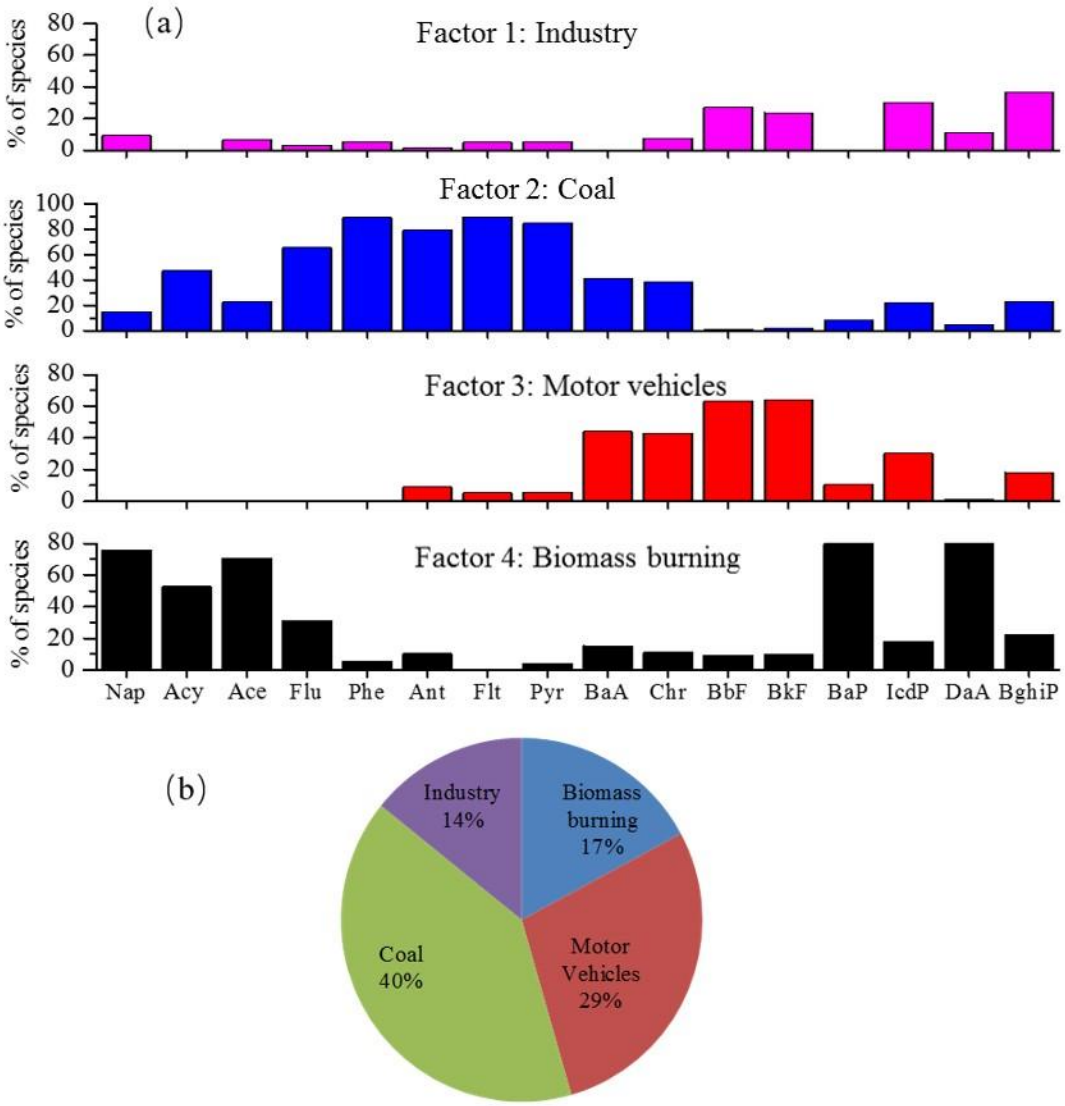

Fig. 6. (a) PAHs source profiles and (b) source contributions derived from PMF

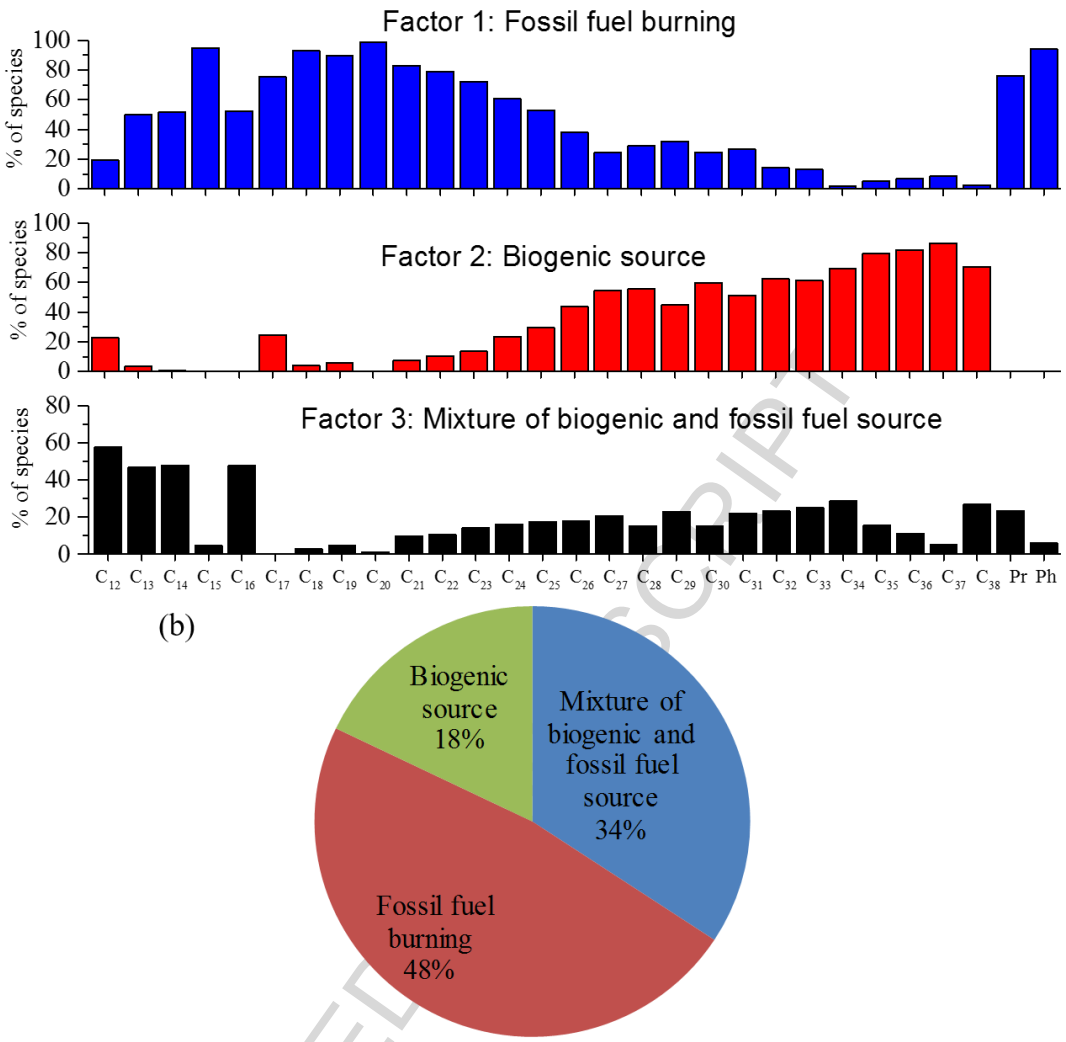

Fig. 7. (a) n-Alkanes source profiles and (b) source contributions derived from PMF

Highlights

- $PM_{2.5}$ and PM_{10} samples were simultaneously collected during four seasons.
- Carbonaceous species (EC, OC, PAHs, and n-alkanes) were quantified and seasonal variations were found.
- Diagnostic ratio and PMF were used to identify the sources of PAHs and n-alkanes.
- Anthropogenic sources including coal combustion and vehicle emission were dominant.